Diagn Interv Radiol 2024; DOI: 10.4274/dir.2023.232466

BREAST IMAGING

ORIGINAL ARTICLE

Diagnostic value of synthetic diffusion-weighted imaging on breast magnetic resonance imaging assessment: comparison with conventional diffusion-weighted imaging

Ebru Yılmaz[1]
Nilgün Güldoğan[1]
Sıla Ulus[2]
Ebru Banu Türk[1]
Mustafa Enes Mısır[3]
Aydan Arslan[4]
Mustafa Erkin Arıbal[3]

[1]Acıbadem Altunizade Hospital Breast Center, Department of Radiology, İstanbul, Türkiye

[2]Acıbadem Ataşehir Hospital, Department of Radiology, İstanbul, Türkiye

[3]Acıbadem Mehmet Ali Aydınlar University, Department of Radiology, İstanbul, Türkiye

[4]University of Health Sciences Türkiye, Ümraniye Training and Research Hospital, Clinic of Radiology, İstanbul, Türkiye

PURPOSE

To compare images generated by synthetic diffusion-weighted imaging (sDWI) with those from conventional DWI in terms of their diagnostic performance in detecting breast lesions when performing breast magnetic resonance imaging (MRI).

METHODS

A total of 128 consecutive patients with 135 enhanced lesions who underwent dynamic MRI between 2018 and 2021 were included. The sDWI and DWI signals were compared by three radiologists with at least 10 years of experience in breast radiology.

RESULTS

Of the 82 malignant lesions, 91.5% were hyperintense on sDWI and 73.2% were hyperintense on DWI. Of the 53 benign lesions, 71.7% were isointense on sDWI and 37.7% were isointense on DWI. sDWI provides accurate signal intensity data with statistical significance compared with DWI ($P < 0.05$). The diagnostic performance of DWI and sDWI to differentiate malignant breast masses from benign masses was as follows: sensitivity 73.1% [95% confidence interval (CI): 62–82], specificity 37.7% (95% CI: 24–52); sensitivity 91.5% (95% CI: 83–96), specificity 71.7% (95% CI: 57–83), respectively. The diagnostic accuracy of DWI and sDWI was 59.2% and 83.7%, respectively. However, when the DWI images were evaluated with apparent diffusion coefficient mapping and compared with the sDWI images, the sensitivity was 92.68% (95% CI: 84–97) and the specificity was 79.25% (95% CI: 65–89) with no statistically significant difference. The inter-reader agreement was almost perfect ($P < 0.001$).

CONCLUSION

Synthetic DWI is superior to DWI for lesion visibility with no additional acquisition time and should be taken into consideration when conducting breast MRI scans. The evaluation of sDWI in routine MRI reporting will increase diagnostic accuracy.

KEYWORDS

Breast tumors, image analysis, diagnostic imaging, diffusion magnetic resonance imaging, echo-planar imaging

Corresponding author: Aydan Arslan

E-mail: arslanaydan@gmail.com

Received 21 August 2023; revision requested 18 September 2023; accepted 22 October 2023.

Epub: 27.10.2023

Publication date: 05.03.2024

DOI: 10.4274/dir.2023.232466

Conventional breast magnetic resonance imaging (MRI) has the highest sensitivity for breast cancer detection, staging of known cancer, and evaluation of response to neoadjuvant chemotherapy. In recent years, specifically according to the Dense Tissue and Early Breast Neoplasm Screening trial[1] and the EA1411 Eastern Cooperative Oncology Group–American College of Radiology (ACR) Imaging Network study,[2] the indication spectrum of breast MRI has widened. The European Society of Breast Imaging now recommends offering screening breast MRI every 2–4 years in women aged 50–70 years with extremely dense breasts.[3] However, MRI is limited by high costs, which include the cost of contrast mate-

You may cite this article as: Yılmaz E, Güldoğan N, Ulus S, et al. Diagnostic value of synthetic diffusion-weighted imaging on breast magnetic resonance imaging assessment: comparison with conventional diffusion-weighted imaging. *Diagn Interv Radiol*. 2024;30(2):91-98.

rial administration, intravenous (IV) supplies, point-of-care renal function screening, and on-site physician coverage for adverse contrast material-related events. Furthermore, prolonged examination time is an additional concern. With the latest concerns regarding the safety of gadolinium-based contrast agents, diffusion-weighted imaging (DWI) has been recommended as an encouraging alternative to dynamic contrast-enhanced MRI for detecting early breast cancer. In addition, an improvement in tumor visibility without contrast injection could improve the cost-effectiveness of MRI. DWI is a fast, widely available, unenhanced MRI technique that provides a unique radiologic image contrast by providing information on the cellular environment of tissues *in vivo*. In recent years, this sequence has been used in addition to conventional sequences and decreases false positivity.

However, DWI has many limitations, such as a decrease in signal-to-noise ratio (SNR) and experiencing eddy current distortions when using a high *b* value; studies have been conducted to overcome these limitations and to improve this sequence.[4] The principal basis for using DWI for disease detection relies on maximizing the image contrast between diseased tissue and the background. The extent to which this occurs depends on the intrinsic tissue diffusivity, the T2 relaxation time, and the diffusion weighting (*b* value) of the motion probing gradients that are applied. The selection of the *b* value is a key point as it directly affects the image SNR, lesion contrast-to-noise ratio, and apparent diffusion coefficients (ADCs). The *b* value can enhance both the lesion detection sensitivity and specificity, but it also leads to a decreased SNR. Furthermore, the perfusion effect is minimized.[5,6] However, acquiring images at higher *b* values (>1.000 sec/mm^2) leads to more distortion due to susceptibility effects and eddy currents and lengthens imaging times.[7-10] One of the new techniques for improving the accuracy of DWI is synthetic DWI (sDWI). sDWI is a mathematical computation technique that builds on previously described principles and calculates a high *b* value (or any *b* value) image from DWI images acquired with at least two different lower *b* values.[11,12] Once the ADC is known, it can be used to extrapolate the expected signal intensity for each image voxel to any computed *b* value using the equation $S(b) = S(0)\, e^{-b*ADC}$, thus generating a computed DWI image.[6,13,14] The calculation of synthetic high *b* values is a strategy to enhance contrast already present in lower *b* value images and is potentially useful to detect and depict lesions but lacks the power of non-Gaussian diffusion to characterize tissues.

sDWI is superior to conventional DWI with fewer artifacts, no inhomogeneity in fat suppression, and a high SNR. There are many reports[15-18] on the efficacy of sDWI for imaging organs such as the prostate; however, there are limited reports on the evaluation of breast lesions.[18,19]

The aim of this study is to investigate the feasibility of the sDWI technique for lesion detection and to compare it with conventional DWI.

Main points

- Synthetic diffusion-weighted imaging (sDWI) is a mathematical computation technique to generate a high *b* value DWI image. No extra acquisition time is required.
- Synthetic DWI is superior to DWI sequence due to fewer artifacts, lack of inhomogeneity in fat suppression, and a high signal-to-noise ratio.
- Synthetic DWI is superior to DWI sequences for lesion visibility, particularly in dense breasts. Thus, sDWI should be considered when conducting breast magnetic resonance imaging scans.

Methods

Patients selection

This study involved a retrospective analysis of acquired data. The medical Ethics Committee of Acıbadem University approved this single institution study (2023-09/303), and informed consent was waived. All the enhancing lesions on breast MRI images between March 2018 and September 2021 were included in the study. The exclusion criteria were as follows: cases with no histopathological diagnosis or 2 years follow-up; cases with biopsy history prior to MRI; cases involving MRI scans following neoadjuvant chemotherapy.

A total of 139 breast MRI scans were evaluated, and four patients were excluded due to artifacts and technical inadequacy (insufficient fat suppression). Consequently, 135 lesions in 128 patients were evaluated (median age: 47.51 ± 11.15 years; age range: 27–79 years). Among these, 117 lesions had histopathological diagnoses, either with core needle biopsy or vacuum-assisted biopsy, and the remaining 18 lesions were stable in the 2-year follow-up and were regarded as benign.

Magnetic resonance imaging technique

All examinations were performed using a 1.5 Tesla (T) MRI device (Aera; Siemens Healthcare) using an 18-channel breast matrix surface receiver coil with prone positioning. Care was taken to perform the MRI scans of premenopausal women between days 5 and 15 of the menstrual cycle. Multiparametric MRI images (fat-sat STIR T2W sequence, a pre-contrast DWI sequence, and a dynamic contrast-enhanced T1W sequence) were obtained for all the patients. For the dynamic contrast-enhanced sequences, 0.1 mmol/kg of body weight of contrast material (Gadovist; Bayer Healthcare Pharmaceutical, Berlin, Germany) was injected. Diffusion-weighted echo-planar images (time of repetition: 3.000–7.000 ms, time of echo: 50–60 ms, field of view: 260–300 mm, matrix: 192 × 192, number of excitations: 1, sectional thickness: 4 mm with a 1 mm intersection gap) were obtained in the axial plane prior to contrast administration. The DWI was obtained using diffusion gradient *b* values of 50–800 sec/mm^2. ADC maps were calculated from raw DWI images using all *b* values and applying the standard monoexponential regression approach performed automatically by the scanner software. sDWI images at *b* = 1.500 sec/mm^2 were automatically constructed in a commercially available workstation using syngo.via VB10 software (Siemens Healthcare, Erlangen, Germany).

Data analysis

The evaluation was performed by three radiologists with at least 10 years of experience in breast radiology. One radiologist evaluated the sDWI images in addition to all sequences, whereas the other two radiologists, who were blinded to the clinical diagnoses and all imaging findings, evaluated only the conventional DWI and sDWI images. Imaging data were analyzed on a dedicated workstation (Multi-Modality Work-Place, Siemens Healthineers). Detection of hyperintense lesions on sDWI and DWI was acknowledged as positive for malignancy suspicion as on DWI, and the readers assigned a qualitative positive or negative assessment.

Lesion size was defined as the largest diameter of the enhancing lesion in the first minute post-contrast T1W sequence. For patients with more than one lesion, the largest lesion was included in the study.

Breast densities were categorized into four groups (type A, B, C, and D) according to the American College of Radiology Breast Imaging Reporting and Data System atlas terminology.[20]

Statistical analysis

Data of continuous variables were presented as a mean ± standard deviation, minimum–maximum, and percentile. A comparison of two variables that were independent and not normally distributed was performed using the Mann–Whitney U test. The chi-squared test (or, when appropriate, Fisher's exact test) was used to investigate the relationship between the categorical variables.

Receiver operating characteristic curve analysis was performed for the determination of ADC cut-off values according to the statistically significant parameters. Subsequently, the diagnostic values and confidence intervals (CIs) were obtained.

The inter-reader agreement was evaluated using intra-class correlation and the Fleiss κ test.

Statistical analysis was performed using MedCalc Statistical Software version 12.7.7 (MedCalc Software bvba, Ostend, Belgium; http://www.medcalc.org; 2013). All *P* values of <0.05 were considered statistically significant.

Results

Eighty-two lesions were malignant (confirmed via histopathologic diagnosis) (mean size: 27.4 ± 20.55 mm, range: 3–100 mm), and 53 lesions were benign (35 lesions were confirmed via histopathologic diagnosis, and 18 lesions were stable in the 2-year follow-up and regarded as benign) (mean size: 13.06 ± 7.66 mm, range: 4–36 mm) (Table 1).

Diagnoses of benign lesions included fibrocystic changes (n = 10; 18.8%), fibroadenoma (n = 7; 13.2%), usual epithelial hyperplasia (n = 1; 1.8%), fat necrosis (n = 2; 3.7%), adenosis (n = 4; 7.5%), stromal fibrosis (n = 8; 15.0%), radial scar (n = 2; 3.7%), intramammary lymph node (n = 1; 1.8%), and stable in the 2-year follow-up (n = 18; 33.9%). Malignant lesion subtypes consisted of invasive ductal carcinoma (IDC) (n = 70; 85.3%), invasive lobular carcinoma (n = 3; 3.6%), metaplastic carcinoma (n = 1; 1.2%), and ductal carcinoma *in situ* (DCIS) (n = 8; 9.7%).

The diagnostic performance of ADC value to differentiate malignant breast masses from benign masses was as follows: sensitivity 92.68% (95% CI: 84–97), specificity 79.25% (95% CI: 65–89), using an ADC cut-off value of 1.189 x 10^{-3} mm^2/sec, which is comparable with the literature data.[21-24]

Of the 82 malignant lesions, 75 were hyperintense on sDWI, whereas 7 were isointense (Figure 1). Four of the 7 sDWI isointense malignant lesions were DCIS. Two of the remaining three IDCs (80 and 10 mm in size and both Luminal B cancers) were located peripherally in the axillary tail, and the lesions were not visualized due to insufficient fat-suppression and distortion in that area (Figure 2). One triple-negative IDC lesion appearing isointense on the DWI image showed diffusion restriction when evaluated with an ADC map. Of the seven isointense cases, six were also isointense on DWI. There was one case in which the biopsy result of DCIS was hyperintense on DWI with a high ADC value (1.504 x 10^{-3} mm^2/sec). Therefore, it was interpreted as no diffusion restriction and DWI hyperintensity may be due to the T2 effect. When the DWIs were evaluated with

Table 1. Summary of characteristics of the study population

Clinical and radiological characteristics		#	
Patient age, median (range) (years)		47.51 ± 11.15 (27–79)	
Amount of fibroglandular tissue (breast density), number (%) of patients	Type A	1 (0.74%)	
	Type B	24 (18.75%)	
	Type C	75 (58.59%)	
	Type D	35 (27.34%)	
Pathology result, number (%) of patients	Malignant	82 (60.74%)	
	Benign	53 (39.25%)	
Lesion size, mean (range)	Benign	13.06 ± 7.66 mm (4–36 mm)	
		Mass	11.18 mm (4–30 mm)
		Non-mass	16.15 mm (6–36 mm)
	Malignant	27.4 ± 20.55 mm (3–100 mm)	
		Mass	25.8 mm (3–80 mm)
		Non-mass	36.5 mm (9–100 mm)
Lesion enhancement patterns (mass, non-mass)		Mass	Non-mass
	Benign	33 (62.26%)	20 (37.73%)
	Malignant	70 (85.36%)	12 (14.63%)

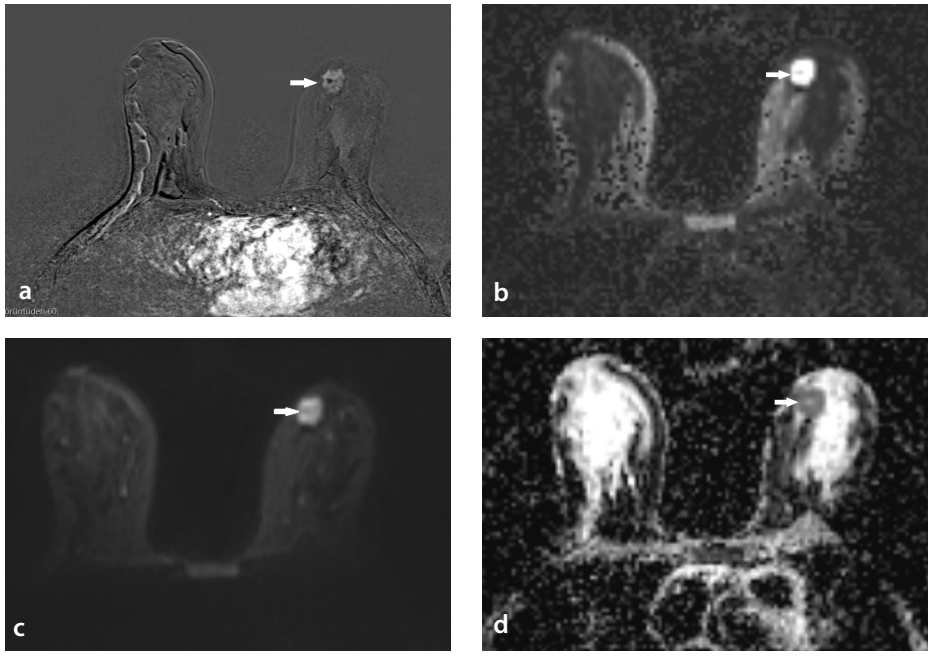

Figure 1. A 44-year-old female patient with a diagnosis of invasive ductal cancer in the inner part of the left breast. In the dynamic contrast-enhanced image **(a)**, there is an irregular mass with heterogeneous enhancement. Synthetic diffusion-weighted image **(b)** showed markedly hyperintense mass, and conventional diffusion-weighted image **(c, d)** showed homogeneous diffusion restriction in the mass (hyperintense on DWI and hypointense on ADC map). The ADC values were measured at least three times. The average ADC value was 0.769 x 10^{-3} mm^2/sec, which is below the cut-off value (1.189 x 10^{-3} mm^2/sec). DWI, diffusion-weighted imaging; ADC, apparent diffusion coefficient.

ADC mapping (using a cut-off value of 1.189 x 10^{-3} mm^2/sec), three cases showed diffusion restriction, whereas four did not (Table 2).

When the stand-alone DWI sequence was evaluated, 60 of the 82 malignant lesions were hyperintense, and the remaining 22 were isointense. Of these 22 isointense lesions, 6 were isointense on both sDWI and DWI, whereas 16 lesions were hyperintense solely on sDWI. When the DWI sequence was compared with ADC mapping, 15 of 16 lesions (in one lesion ADC value is 1.239 mm^2/sec) showed restricted diffusion with ADC values less than the cut-off value of 1.189 x 10^{-3} mm^2/sec.

Comparison of DWI acquired with b = 800 diffusion gradient to sDWI at b = 1.500 value (Table 3) in the detection of malignant lesions showed that sDWI was significantly effective ($P < 0.001$).

Of the 53 benign lesions, 38 were isointense on sDWI, whereas 15 were hyperintense (Figure 3). Of these 15 hyperintense lesions, 4 were isointense on DWI and the remaining 11 were hyperintense (Table 4). When compared with ADC mapping, 6 of these 11 lesions had ADC values above the cut-off value of 1.189 x 10^{-3} mm^2/sec. The remaining 5 lesions had ADC values below the cut-off value.

For the 53 benign lesions, 33 were hyperintense, and 20 were isointense on DWI images. ADC mapping showed values below the cut-off value of 1.189 x 10^{-3} mm^2/sec in 11 of these 53 benign lesions.

When the sDWI and DWI sequences for benign lesions were compared, the false positivity rates were 28.30% and 62.26%, respectively. If DWI sequences are assessed in conjunction with the ADC map, the rate of false positive results is 20.75%.

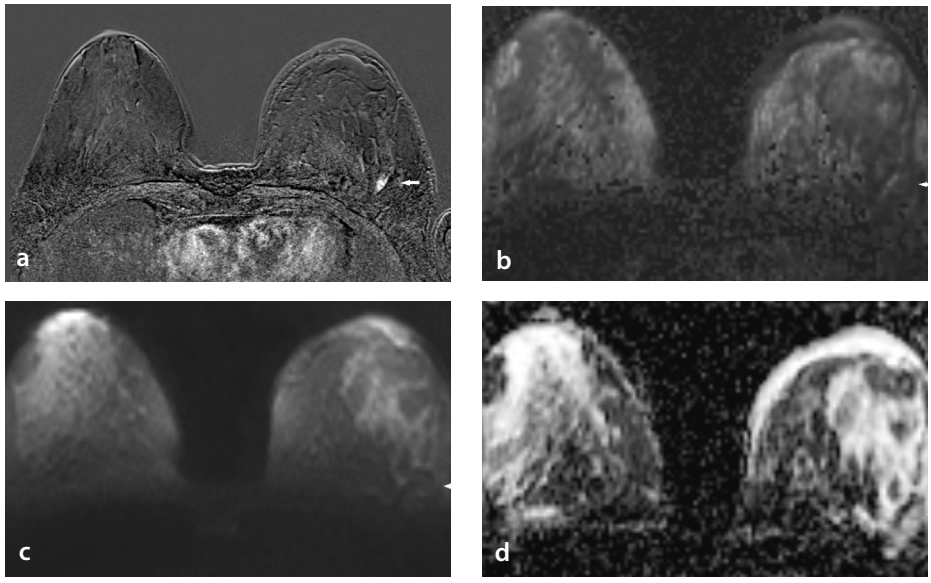

Figure 2. A 64-year-old female patient with a diagnosis of Luminal B IDC in the axillary tail of the left breast is observed. In the dynamic contrast-enhanced image **(a)**, there is an enhanced non-mass lesion, which is a potential malignancy. Synthetic diffusion-weighted image **(b)** showed lesion isointense. Conventional diffusion-weighted image **(c)** showed lesion isointense and DWI was evaluated with ADC map **(d)** there is diffusion restriction in the lesion. The average ADC value was 1.003 x 10^{-3} mm^2/sec, which is below the cut-off value (1.189 x 10^{-3} mm^2/sec). IDC, invasive ductal carcinoma; DWI, diffusion-weighted imaging; ADC, apparent diffusion coefficient.

Table 2. Analysis of the seven false (-) lesions on sDWI

Maximum diameter	Pathology result	DWI	ADC value (x10^{-3} mm^2/sec)	sDWI
15 mm	DCIS	Isointense	1.156*	Isointense
10 mm	Luminal B IDC	Isointense	1.003*	Isointense
80 mm	Luminal B IDC	Isointense	1.328	Isointense
10 mm	DCIS	Isointense	1.514	Isointense
12 mm	DCIS	Isointense	1.200	Isointense
10 mm	Triple (-) IDC	Isointense	1.184*	Isointense
23 mm	DCIS	Hyperintense	1.504	Isointense

*The ADC values below the cut-off (1.189 x 10^{-3} mm^2/sec) are marked. DWI, diffusion-weighted imaging; ADC, apparent diffusion coefficient; sDWI, synthetic diffusion-weighted imaging; IDC, invasive ductal carcinoma; DCIS, ductal carcinoma *in situ*.

Table 3. Comparison of lesion signal intensities of DWI obtained with b = 800 diffusion gradient and sDWI with b = 1.500

Pathology result		Benign		Malignant		*P* value			
		n	%	n	%				
DWI	Hyperintense	33	62.3%	60	73.2%	0.189			
	Isointense	20	37.7%	22	26.8%				
sDWI	Hyperintense	15	28.3%	75	91.5%	<0.001			
	Isointense	38	71.7%	7	8.5%				
Pathology result		Benign		Malignant					
n		%	n	%	Auc	Acc	Sensitivity	Specificity	
DWI	Hyperintense	20	37.7%	22	26.8%	0.555	0.592	0.731 (0.622–0.824)	0.377 (0.248–0.521)
	Isointense	33	62.3%	60	73.2%				
sDWI	Hyperintense	38	71.7%	7	8.5%	0.816	0.837	0.915 (0.832–0.965)	0.717 (0.576–0.832)
	Isointense	15	28.3%	75	91.5%				

DWI, diffusion-weighted imaging; sDWI, synthetic diffusion-weighted imaging; AUC, area under curve; Acc, accuracy.

The diagnostic performance of DWI and sDWI to differentiate malignant breast masses from benign masses was as follows: sensitivity 73.1% (95% CI: 62–82), specificity 37.7% (95% CI: 24–52); sensitivity 91.5% (95% CI: 83–96), specificity 71.7% (95% CI: 57–83), respectively. The diagnostic accuracy of DWI and sDWI was 59.2% and 83.7%, respectively.

Lesion size represents a significant limitation when evaluating lesions on the DWI sequence. In this investigation, a total of seven malignant lesions were identified that appeared isointense in the sDWI sequence, rendering them undetectable. These lesions displayed a size range spanning from 10–80 mm, with an average size of 22.85 mm. Within the DWI sequence, 22 out of 82 malignant lesions exhibited isointensity and remained undetectable. These lesions varied in size from 9–80 mm, with an average size of 23.54 mm. Notably, there was one lesion measuring <1 cm (9 mm) that could not be detected in the DWI sequence.

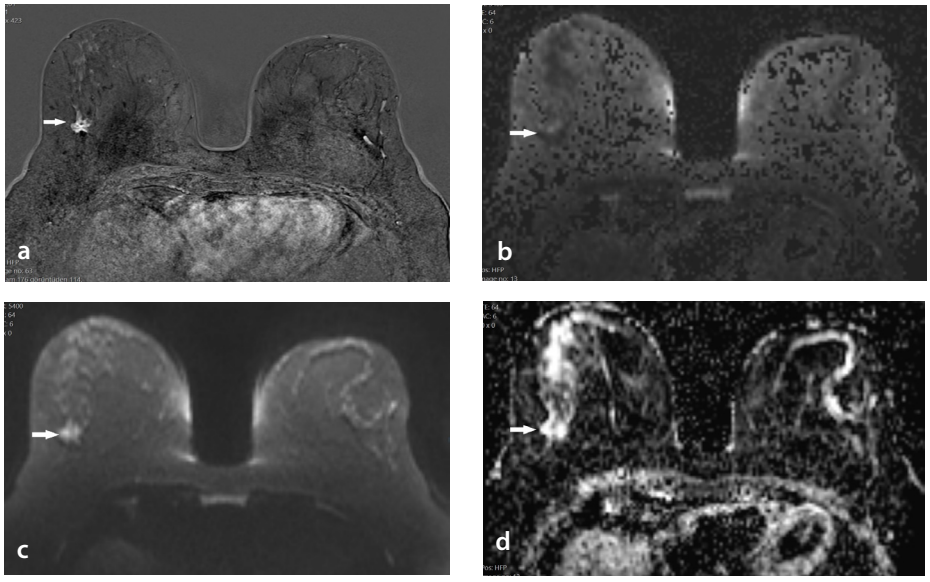

Figure 3. A 42-year-old female patient with a diagnosis of stromal fibrosis in the outer part of the right breast was observed. Structural distortion was observed on routine annual mammography and MRI was suggested. In the dynamic contrast-enhanced image **(a)**, there was an enhanced lesion with an irregular shape, which indicates malignancy. The synthetic diffusion-weighted image **(b)** showed lesion isointense. The conventional diffusion-weighted image **(c)** showed a hyperintense signal but when DWI was evaluated with an ADC map **(d)** there was no diffusion restriction in the lesion. The average ADC value was 1.429 x 10^{-3} mm^2/sec, which is above the cut-off value (1.189 x 10^{-3} mm^2/sec). MRI, magnetic resonance imaging; DWI, diffusion-weighted imaging; ADC, apparent diffusion coefficient.

In addition, the study identified a total of 32 lesions falling within the size range of 3–9 mm (<1 cm). Among these, 9 were malignant and 23 were benign. As explained earlier, all but one of these nine malignant lesions were detectable. Among the benign lesions, 11 displayed isointensity in both sequences, 7 showed hyperintensity solely in the DWI sequence, and 6 were hyperintense in both the DWI and sDWI sequences. When comparing the relationship between size and detectability in both benign and malignant lesions, no statistically significant difference ($P = 0.0867$) was found. These findings suggest that size does not significantly impact the assessment of lesions in the DWI and sDWI sequences.

The distribution of the individual amounts of fibroglandular tissue (FGT) is important because difficulties with lack of fat saturation are more common in breasts with a high percentage of fat.[12] The performance of DWI and sDWI sequences can be affected by the distribution of FGT. In this study, the composition of the female group included 24 (18.75%) women within ACR category B, 75 (58.59%) women within category C, and 35 (27.34%) women within category D. Only one case was categorized as "type A," and this category was thus disregarded (shown in Table 5). No statistically significant difference was found between the breast parenchymal distribution and signal distribution DWI and sDWI sequences regarding type B, type C, and type D (DWI $P = 0.066$; sDWI $P = 0.335$).

Table 4. Analysis of the 15 false (+) lesions on sDWI

Maximum diameter	Pathology result	DWI	ADC (x10^{-3} mm^2/sec)	sDWI
12 mm	Radial scar	Hyperintense	1.077*	Hyperintense
30 mm	Fibrocystic change	Hyperintense	1.218	Hyperintense
27 mm	Fibrocystic change	Hyperintense	1.614	Hyperintense
9 mm	Stabil -2 years follow up	Hyperintense	1.409	Hyperintense
9 mm	Stabil -2 years follow up	Hyperintense	1.460	Hyperintense
5 mm	Stabil -2 years follow up	Hyperintense	1.357	Hyperintense
8 mm	Intramammary lymph node	Hyperintense	1.100*	Hyperintense
8 mm	Apocrine metaplasia	Hyperintense	1.309	Hyperintense
30 mm	Adenosis	Isointense	1.112*	Hyperintense
12 mm	Stromal fibrosis	Isointense	1.016*	Hyperintense
13 mm	Fibroadenoma	Isointense	1.122*	Hyperintense
30 mm	Sclerosing adenosis	Isointense	1.079*	Hyperintense
36 mm	Apocrine metaplasia.fibrocystic change	Hyperintense	1.033*	Hyperintense
24 mm	Complex sclerosing lesion	Hyperintense	1.152*	Hyperintense
13 mm	Usual epithelial hyperplasia	Hyperintense	0.928*	Hyperintense

*The ADC values below the cut-off (1.189 x 10^{-3} mm^2/sec) are marked. DWI, diffusion-weighted imaging; ADC, apparent diffusion coefficient; sDWI, synthetic diffusion-weighted imaging.

Synthetic DWI inter-reader agreement was almost perfect for lesion visibility (shown in Table 6) and was statistically significant (κ: 0.922, $P < 0.001$).

Discussion

DWI has been proposed as an unenhanced option for breast cancer screening via MRI, and synthetic *b* values may improve lesion visibility without increasing the acquisition time while avoiding the disadvantages of performing DWI at extremely high *b* values. In this study, DWI was assessed for tumor visibility and breast cancer detection by a combination of acquired *b* values (800 sec/mm^2), ADC maps, and synthetic *b* values (1.500 sec/mm^2). Synthetic *b* values of 1.500 sec/mm^2 provided the best lesion conspicuity. Benign lesions were more conspicuous at lower *b* values, whereas malignant tumors appeared brighter than the surrounding parenchyma at higher *b* values, particularly in breast composition categories C and D, where lesions can be masked on mammograms by the density of FGT. The study shows that sDWI sequences are superior to DWI sequences for lesion visibility, and the results corroborate those in the recent literature.[11,18]

In this study, the lesion visibility was assessed using DWI and sDWI. The former was significantly less sensitive than the latter (73.1% vs. 91.5%, $P < 0.001$). Furthermore, the detection rate of cancer was not significantly different when the DWI sequences were evaluated in conjunction with ADC mapping (92.68%). In two independent studies,[11,18] the conventional DWI of cancer to parenchyma contrast ratio of malignant lesions was compared with DWI with higher *b* values. The authors reported that the tumor-to-parenchymal contrast ratio of sDWI was significantly higher than that of conventional DWI, without compromising the cancer detection rate. In another study, Blackledge et al.[16] claimed that sDWI raised the rate of lesion detection in comparison to DWI. O'Flynn et al.[19] also reported that sDWI increased sensitivity for breast cancer. However, these studies involved smaller cohorts, and only malignant lesions were evaluated.

The prime focus of DWI is to differentiate between benign and malignant lesions to prevent unnecessary breast biopsies or enable screening without admission of IV contrast media. Only 19%–36% of the lesions that are biopsied due to MR examination results turn out to be malignant.[25,26] It is particularly important to differentiate benign lesions, which show contrast enhancement resulting in false positive results. There is limited data on the evaluation of benign lesions on sDWI.[18] Unlike other studies, in this study, both malignant and benign lesions were evaluated. The rate of false positivity of sDWI and DWI was 28.30% and 62.26%, respectively. The high rate of false positivity on DWI has been attributed to the T2 shine-through effect.[16] However, the false positivity was 20.75% when DWI was evaluated with an ADC map (Table 2). This data indicates that by first examining the sDWI images and then evaluating any questionable lesions using the ADC map, the opportunity exists to achieve a quicker and more precise diagnosis, while also avoiding unnecessary biopsies.

Studies conducted in recent years have shown that the combined evaluation of early phase contrast images and DWI can replace late-phase and kinetic-curve evaluation, meaning results can be achieved with a much shorter imaging time.[27] Furthermore, in recent years, an annual or biannual screening MRI has been recommended for high-risk patients with dense breasts, and an abbreviated MRI is aimed at achieving fast and accurate results.[28] The primary objective of breast MRI is to enhance the precision of diagnosis while minimizing the likelihood of overdiagnosis. In most of the abbreviated MRI protocols, DWI sequences are included.[29-31] This study shows that adding sDWI scans, which do not require additional acquisition time in the evaluation, has the potential to increase the diagnostic accuracy of abbreviated MRI evaluations.

The performance of DWI and sDWI sequences can be affected by the distribution of FGT. Fat suppression cannot be made homogeneously in fatty breasts in diffusion-weighted sequences. Furthermore, fatty breasts have a lower ADC value compared with dense breasts in the retroareolar region and upper outer quadrant.[12,32] This study did not identify any correlation between breast density and the detectability of lesions on either DWI or sDWI. Similarly, prior studies[32,33] showed that the visibility of breast lesions on DWI was not influenced by breast density. However, since the optimal evaluation is often made with mammography in women with fatty breasts, MRI is rarely required for the evaluation of the patient and thus, the number of fatty breasts in the study group is extremely low.

This study has a number of limitations. First, it is a single-center study. A multicentral study will be valuable to showing the reproducibility of the findings. Second, this study evaluated only lesion detection. Although the image quality in the sDWI series is relatively high, no quantitative assessment was conducted. Furthermore, the role of DWI in the visualization of non-mass enhancement is not definite.[34-36] In this study, this patient group was not evaluated separately; this evaluation should be conducted in further studies.

Table 5. Cross-evaluation of the relationship between signal distribution and breast parenchyma compositions in DWI and sDWI sequences

		Breast density category						
		Type B		Type C		Type D		
		n	%	n	%	n	%	*P* value
B800	Hyperintense	20	83.3	53	70.7	20	57.1	0.066
	Isointense	4	16.7	22	29.3	15	42.9	
B1500	Hyperintense	16	66.7	48	64.0	26	74.3	0.335
	Isointense	8	33.3	27	36.0	9	25.7	

DWI, diffusion-weighted imaging; sDWI, synthetic diffusion-weighted imaging.

Table 6. Inter-reader agreement assessment

Readers	sDWI signal assesment	n (number of patients)	%	κ (kappa)	*P* value
Reader 1	Hyperintense	90	66.7	0.922	<0.001
	Isointense	45	33.3		
Reader 2	Hyperintense	90	66.7		
	Isointense	45	33.3		
Reader 3	Hyperintense	91	67.4		
	Isointense	44	32.6		

sDWI, synthetic diffusion-weighted imaging.

To conclude, the findings indicate that sDWI exhibits significantly greater sensitivity than conventional DWI in assessing both malignant and benign lesions. The results indicate that the inclusion of sDWI image evaluation in the interpretation of breast MRI scans has the potential for a better outcome.

Conflict of interest disclosure

The authors declared no conflicts of interest.

References

1. Bakker MF, de Lange SV, Pijnappel RM, et al. Supplemental MRI screening for women with extremely dense breast tissue. *N Engl J Med*. 2019;381(22):2091-2102. [CrossRef]
2. Rahbar H, Zhang Z, Chenevert TL, et al. Utility of diffusion-weighted imaging to decrease unnecessary biopsies prompted by breast MRI: a trial of the ECOG-ACRIN Cancer Research Group (A6702). *Clin Cancer Res*. 2019;25(6):1756-1765. [CrossRef]
3. Mann RM, Athanasiou A, Baltzer PAT, et al. Breast cancer screening in women with extremely dense breasts recommendations of the European Society of Breast Imaging (EUSOBI). *Eur Radiol*. 2022;32(6):4036-4045. [CrossRef]
4. Baltzer PA, Benndorf M, Dietzel M, Gajda M, Camara O, Kaiser WA. Sensitivity and specificity of unenhanced MR mammography (DWI combined with T2-weighted TSE imaging, ueMRM) for the differentiation of mass lesions. *Eur Radiol*. 2010;20(5):1101-1110. [CrossRef]
5. Le Bihan D, Breton E. Imagerie de diffusion in vivo par résonance magnétique. *C R Acad Sci (Paris)*. 1985;301(15):1109-1111. [CrossRef]
6. Le Bihan D, Breton E, Lallemand D, Aubin ML, Vignaud J, Laval-Jeantet M. Separation of diffusion and perfusion in intravoxel incoherent motion MR imaging. *Radiology*. 1988;168(2):497-505. [CrossRef]
7. Katahira K, Takahara T, Kwee TC, et al. Ultrahigh-b-value diffusion-weighted MR imaging for the detection of prostate cancer: evaluation in 201 cases with histopathological correlation. *Eur Radiol*. 2011;21(1):188-196. [CrossRef]
8. Kitajima K, Kaji Y, Kuroda K, Sugimura K. High b-value diffusion-weighted imaging in normal and malignant peripheral zone tissue of the prostate: effect of signal-to-noise ratio. *Magn Reson Med Sci*. 2008;7(2):93-99. [CrossRef]
9. Nilsson M, Szczepankiewicz F, van Westen D, Hansson O. Extrapolation-based references improve motion and eddy-current correction of high B-value DWI data: application in Parkinson's disease dementia. *PLoS One*. 2015;10(11):e0141825. [CrossRef]
10. Amornsiripanitch N, Bickelhaupt S, Shin HJ, et al. Diffusion-weighted MRI for unenhanced breast cancer screening. *Radiology*. 2019;293(3):504-520. [CrossRef]
11. Bickel H, Polanec SH, Wengert G, et al. Diffusion-weighted MRI of breast cancer: improved lesion visibility and image quality using synthetic b-values. *J Magn Reson Imaging*. 2019;50(6):1754-1761. [CrossRef]
12. Naranjo ID, Lo Gullo R, Saccarelli C, et al. Diagnostic value of diffusion-weighted imaging with synthetic b-values in breast tumors: comparison with dynamic contrast-enhanced and multiparametric MRI. *Eur Radiol*. 2021;31(1):356-367. [CrossRef]
13. Blackledge MD, Wilton B, Messiou C, Koh DM, Leach MO, Collins DJ. Computed diffusion weighted imaging (cDWI) for improving imaging contrast [abstr]. In: Proceedings of the International Society for Magnetic Resonance in Medicine. Berkeley, Calif: International Society for Magnetic Resonance in Medicine. 2009; 4005. [CrossRef]
14. Blackledge MD, Collins DJ, Koh DM, Leach MO. SNR of high b-value diffusion weighted images can be improved using cDWI [abstr]. In: Proceedings of the International Society for Magnetic Resonance in Medicine. Berkeley, Calif: International Society for Magnetic Resonance in Medicine. 2010; 4707. [CrossRef]
15. Kawahara S, Isoda H, Fujimoto K, et al. Additional benefit of computed diffusion-weighted imaging for detection of hepatic metastases at 1.5T. *Clin Imaging*. 2016;40(3):481-485. [CrossRef]
16. Blackledge MD, Leach MO, Collins DJ, Koh DM. Computed diffusion-weighted MR imaging may improve tumor detection. *Radiology*. 2011;261(2):573-581. [CrossRef]
17. Park JH, Yun B, Jang M, et al. Comparison of the diagnostic performance of synthetic versus acquired high b-value (1500 s/mm^2) diffusion-weighted MRI in women with breast cancers. *J Magn Reson Imaging*. 2019;49(3):857-863. [CrossRef]
18. Choi BH, Baek HJ, Young Ha J, et al. Feasibility study of synthetic diffusion-weighted MRI in patients with breast cancer in comparison with conventional diffusion-weighted MRI. *Korean J Radiol*. 2020;21(9):1036-1044. [CrossRef]
19. O'Flynn EA, Blackledge M, Collins D, et al. Evaluating the diagnostic sensitivity of computed diffusion-weighted MR imaging in the detection of breast cancer. *J Magn Reson Imaging*. 2016;44(1):130-137. [CrossRef]
20. Sickles EA, D'Orsi CJ, Bassett LW. ACR BI-RADS Mammography. In: ACR BI-RADS Atlas, Breast Imaging Reporting and Data System, 5th ed. American College of Radiology, Reston, VA; 2013. [CrossRef]
21. Şahin, C, Arıbal E. The role of apparent diffusion coefficient values in the differential diagnosis of breast lesions in diffusion-weighted MRI. *Diagn Interv Radiol*. 2013;19(6):457-462. [CrossRef]
22. Yılmaz E, Sarı O, Yılmaz A, et al. Diffusion-weighted imaging for the discrimination of benign and malignant breast masses; utility of ADC and relative ADC. *J Belg Soc Radiol*. 2018;102(1):24. [CrossRef]
23. Yılmaz E, Erok B, Atca AÖ. Measurement of the apparent diffusion coefficient in discrimination of benign and malignant axillary lymph nodes. *Pol J Radiol*. 2019;84:592-597. [CrossRef]
24. Baltzer P, Mann RM, Lima M, et al. Diffusion-weighted imaging of the breast-a consensus and mission statement from the EUSOBI International Breast Diffusion-Weighted Imaging Working Group. *Eur Radiol*. 2020;30(3):1436-1450. [CrossRef]
25. Harvey JA, Hendrick RE, Coll JM, Nicholson BT, Burkholder BT, Cohen MA. Breast MR imaging artifacts: how to recognize and fix them. *Radiographics*. 2007;27(Suppl 1):131-145. [CrossRef]
26. Strigel RM, Rollenhagen J, Burnside ES, et al. Screening breast MRI outcomes in routine clinical practice: comparison to BI-RADS benchmarks. *Acad Radiol*. 2017;24(4):411-417. [CrossRef]
27. Dietzel M, Ellmann S, Schulz-Wendtland R, et al. Breast MRI in the era of diffusion-weighted imaging: do we still need signal-intensity time curves? *Eur Radiol*. 2020;30(1):47-56. [CrossRef]
28. Comstock CE, Gatsonis C, Newstead GM, et al. Comparison of abbreviated breast MRI vs digital breast tomosynthesis for breast cancer detection among women with dense breasts undergoing screening. *JAMA*. 2020;323(8):746-756. [CrossRef]
29. Jain M, Jain A, Hyzy MD, Werth G. FAST MRI breast screening revisited. *J Med Imaging Radiat Oncol*. 2017;61(1):24-28. [CrossRef]
30. Kang JW, Shin HJ, Shin KC, et al. Unenhanced magnetic resonance screening using fused diffusion-weighted imaging and maximum-intensity projection in patients with a personal history of breast cancer: role of fused DWI for postoperative screening. *Breast Cancer Res Treat*. 2017;165(1):119-128. [CrossRef]
31. Yamada T, Kanemaki Y, Okamoto S, Nakajima Y. Comparison of detectability of breast cancer by abbreviated breast MRI based on diffusion-weighted images and postcontrast MRI. *Jpn J Radiol*. 2018;36(5):331-339. [CrossRef]
32. Hahn SY, Ko ES, Han BK, Lim Y, Gu S, Ko EY. Analysis of factors influencing the degree of detectability on diffusion-weighted MRI and diffusion background signals in patients with invasive breast cancer. *Medicine (Baltimore)*. 2016;95(27):e4086. [CrossRef]

33. Iacconi C, Thakur SB, Dershaw DD, Brooks J, Fry CW, Morris EA. Impact of fibroglandular tissue and background parenchymal enhancement on diffusion weighted imaging of breast lesions. *Eur J Radiol*. 2014;83(2):2137-2143. [CrossRef]

34. Kul S, Eyuboglu I, Cansu A, Alhan E. Diagnostic efficacy of the diffusion weighted imaging in the characterization of different types of breast lesions. *J Magn Reson Imaging*. 2014;40(5):1158-1164. [CrossRef]

35. Imamura T, Isomoto I, Sueyoshi E, et al. Diagnostic performance of ADC for non-mass-like breast lesions on MR imaging. *Magn Reson Med Sci*. 2010;9(4):217-225. [CrossRef]

36. Yabuuchi H, Matsuo Y, Kamitani T, et al. Non-mass like enhancement non contrast-enhanced breast MR imaging: lesion characterization using combination of dynamic contrast-enhanced and diffusion-weighted MR images. *Eur J Radiol*. 2010;75(1):126-132. [CrossRef]